Huang, D.M.; Chandler, D.
Cavity formation and the drying transition in the Lennard-Jones fluid, *Physical Review E*, 2000; 61(2):1501-1506

http://journals.aps.org/pre/abstract/10.1103/PhysRevE.61.1501

Cavity formation and the drying transition in the Lennard-Jones fluid

David M. Huang and David Chandler*
Department of Chemistry, University of California at Berkeley, Berkeley, California 94720
(Received 3 September 1999)

By simulation and theory, we study the probability of observing N molecular centers within molecular sized volumes for a Lennard-Jones fluid near liquid-vapor coexistence. For large volumes and small N, the probability distribution differs markedly from Gaussian. The free energy per unit surface area to form empty volumes (i.e., cavities) is a rapidly varying function of the radius for small cavities. It becomes constant for large volumes. The source of these behaviors is the occurrence of drying (i.e., solvent depletion) at the cavity surface. The crossover to drying occurs on microscopic length scales, with significant density depletion found for cavities with radii of the order of two or more Lennard-Jones diameters. Reasonable agreement is found between the simulation results and the theory developed by Lum, Chandler, and Weeks [J. Phys. Chem. B **103**, 4570 (1999)].

PACS number(s): 61.20.Gy, 61.20.Ja, 61.20.Ne, 68.45.−v

I. INTRODUCTION

Under conditions at which the liquid is the stable phase for a bulk fluid, the presence of a large solute can produce competing surface energetics favoring the metastable vapor phase, thereby inducing drying, or depletion of solvent, near the solute surface. Solvent depletion near surfaces has been observed, for example, in simulations of nanometer sized plates in water [1], in simulations of hard spheres with attractive Lennard-Jones interactions near a hard wall [2], in simulations of a lattice gas confined between two walls [3], and in simulations of the mathematically isomorphic Ising wetting transition [4]. Surface drying has been invoked as a possible reason for the strong attractive forces measured experimentally between hydrophobic plates in water [5]. The nanometer length scale on which drying occurs in that liquid [1,6] is a hydrophobic length scale of relevance to structural biology [7]. Drying may therefore be important in a proper thermodynamic description of protein folding and stability. While this particular possibility remains to be investigated, it is clear that surface induced drying is a phenomenon of general importance and is thus a topic of theoretical interest.

Lum, Chandler, and Weeks (LCW) have recently developed a theory of such drying that captures both small and large length scale effects [6]. The LCW treatment, a statistical field theory version of the density functional theory due to Weeks, Katsov, and Vollmayr [8], provides a means of interpreting solute induced drying in terms of the properties of the pure liquid. The LCW theory was developed to understand the effects of hydrophobic solutes. It applies more generally, however, and it can be used to study surface induced drying for solvation processes occurring in any liquid, not just water.

In this paper, we study surface induced drying in the Lennard-Jones fluid by computer simulation and we compare our simulation results with the predictions of LCW theory. We do so by following the perspective invented by Pratt and his co-workers [9–11]. In particular, we determine the statistics of occupation probabilities of spherical volumes. The probability of zero occupation corresponds to the probability of finding a cavity or void in a liquid. In a liquid close enough to phase coexistence, the surface of a large enough cavity can induce drying. The Lennard-Jones (LJ) fluid is sufficiently simple to make simulations computationally efficient. Furthermore, its equation of state [12] and surface tension [13,14], required as input for the LCW theory, are accurately known. Its uniform fluid radial distribution function, also used in LCW theory, is easily estimated [15].

II. COMPUTER SIMULATIONS

We performed constant pressure Monte Carlo simulations for the LJ fluid with the potential truncated and shifted at 2.5σ. The interaction pair potential is

$$u_{\mathrm{LJT}}(r)=u_{\mathrm{LJ}}(r)-u_{\mathrm{LJ}}(2.5\sigma), \qquad r\leqslant 2.5\sigma,$$
$$=0, \qquad r>2.5\sigma, \tag{1}$$

where

$$u_{\mathrm{LJ}}(r)=4\varepsilon\left[\left(\frac{\sigma}{r}\right)^{12}-\left(\frac{\sigma}{r}\right)^{6}\right]. \tag{2}$$

In most cases, a system of 864 particles was simulated. The reduced temperature $T^*=k_BT/\varepsilon$ and pressure $p^*=p\sigma^3/\varepsilon$ were 0.85 and 0.022, respectively. This corresponds to a reduced density $\rho^*=\rho\sigma^3$ of 0.70, which is the bulk liquid density n_l referred to later. This thermodynamic state is an example of a liquid close to liquid-vapor coexistence, sufficiently close that surface induced drying can occur.

Each simulation was directed towards computing the probability $P(N;v)$ that N particles can be found in a spherical volume $v=4\pi R^3/3$. Volumes with radii R from 0.5 to 3.0σ were considered. The excess chemical potential of a spherical cavity with volume v, $\Delta\mu_v$, is related to this probability by [9]

*Author to whom correspondence should be addressed. Electronic address: chandler@cchem.berkeley.edu

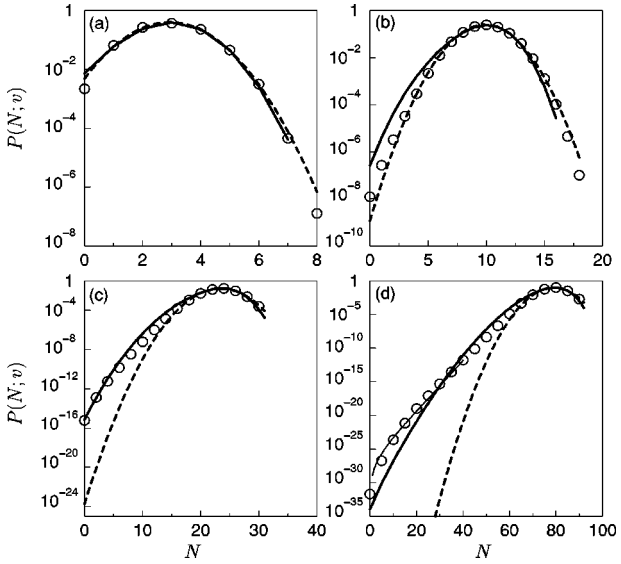

FIG. 1. Volume occupation probabilities $P(N;\,v)$ for LJ fluid ($\rho^*=0.70$, $T^*=0.85$, $p^*=0.022$) from simulation (circles), from the Gaussian distribution with mean occupancy $\langle N\rangle_v$ and variance $\langle N^2\rangle_v-\langle N\rangle_v^2$ (dashed lines), and from LCW theory (thick solid lines). The radii are (a) 1.0σ, (b) 1.5σ, (c) 2.0σ, and (d) 3.0σ. Fit of Eq. (7) to the simulation curve is shown in (d) (thin solid line).

$$\Delta\mu_v=-k_BT\ln P(0;v). \tag{3}$$

The term *cavity* refers to an empty volume, i.e., a volume with $N=0$. Straightforward simulations provide statistically accurate data about small fluctuations around the mean volume occupancy. Large fluctuations are very improbable. To obtain statistics for large fluctuations, umbrella sampling [16] was used. Sampling was carried out with overlapping windows, each containing approximately 8 values of N. Within each window, a weight function was used to bias the $P(N;v)$ distribution. A conventional simulation confined to the window was first performed to obtain an estimate of the distribution in that window. The weight function, $\tilde{w}(N)$ for the umbrella sampled simulation was then chosen to be $\tilde{w}(N)\propto 1/P_{\rm est}(N;v)$, where $P_{\rm est}(N;v)$ is the estimated distribution. This choice for $\tilde{w}(N)$ produced a nearly uniform distribution of N within that window, thus enabling it to be efficiently sampled. During each simulation, the system was equilibrated for 100 000 Monte Carlo cycles, and data was collected every 5 cycles for a total of 200 000 cycles. Error estimates for all our simulation results are no larger than half the size of the circles we use to graphically represent the results in Figs. 1–3.

For the $R=3.0\sigma$ volume, the average side length of the simulation box was less than twice the volume diameter. To investigate the significance of finite size effects, the simulations were repeated for a system of 2048 particles, corresponding to an increase in box side length of 33%. No significant change to the calculated probability distributions or excess chemical potentials was found. This finding indicates that, for the results reported herein, finite size effects are not important in the 864 particle system.

The $P(N;v)$ distributions computed from simulation are shown in Fig. 1. Gaussians with the same mean and variance as these distributions are also plotted. Gaussian statistics of density fluctuations is the basis of the most successful theories of microscopic structure of uniform fluids [17]. It is clear from Fig. 1 that, although the distributions are very close to Gaussian for the smaller volumes, they deviate significantly from Gaussian behavior for large volumes and small N. For the $R=3.0\sigma$ volume, the Gaussian distribution underestimates $P(0;v)$ by 50 orders of magnitude, corresponding to an overestimate of the excess cavity chemical potential $\Delta\mu_v$ of more than $100k_BT$. Predictions of the thermodynamics of solvation of large objects based on Gaussian statistics for $P(N;v)$ are therefore likely to yield erroneous results, as illustrated in Fig. 2.

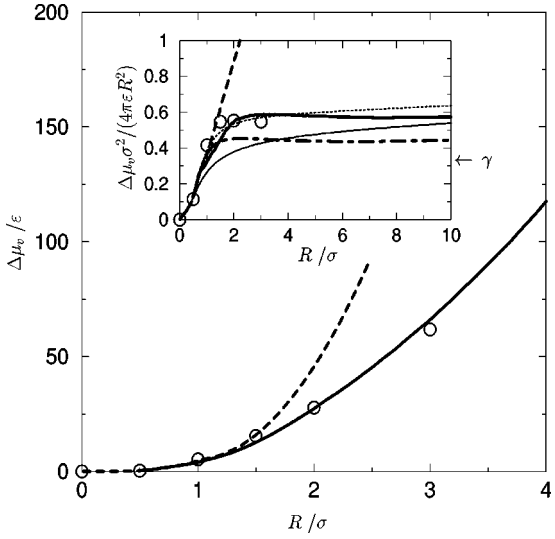

FIG. 2. Excess chemical potential for a cavity of radius R in the LJ fluid ($\rho^*=0.70$, $T^*=0.85$, $p^*=0.022$) from simulation (circles), from the Gaussian distribution with mean occupancy $\langle N\rangle_v$ and variance $\langle N^2\rangle_v-\langle N\rangle_v^2$ (dashed line), and from LCW theory (thick solid line). Inset is the excess chemical potential per unit surface area of the sphere. The arrow indicates the value of the surface tension γ for the nearby coexisting liquid and vapor [13]. Also shown in the inset are the scaled particle theory results using the Reiss approximation [18] (thin solid line) and the Stillinger approximation [19] with surface tension values of $0.33\varepsilon/\sigma^2$ (dot-dash line) and $0.56\varepsilon/\sigma^2$ (dotted line).

Figure 3 shows the average particle density, $n(\mathbf{r})$, as a function of the distance r from a spherical cavity center at the origin. Specifically, $g(r+R)=n(r+R)/n_l$ is plotted for cavities with radii $R=1.0$, 2.0, and 3.0σ. The contact value, $g(R^+)$, can be related to the compressive force $\partial\Delta\mu_v/\partial R$ exerted on the cavity by the surrounding solvent [18]. In particular,

$$\frac{\partial\Delta\mu_v}{\partial R}=4\pi n_lk_BTR^2g(R^+). \tag{4}$$

Stillinger [19] argued that for cavities in water, $g(R^+)$ is a nonmonotonic function of R. With the same reasoning, essentially the same behavior is expected and observed in the current work for the LJ fluid. For small cavities, $g(R^+)$ increases from 1.0 for a cavity of zero radius as the surrounding fluid, acting as a locally elastic medium, applies an increasing compressive force. For the $R=1.0\sigma$ cavity, $g(R^+)>1.0$. Density depletion, i.e., $g(R^+)<1.0$, is evident

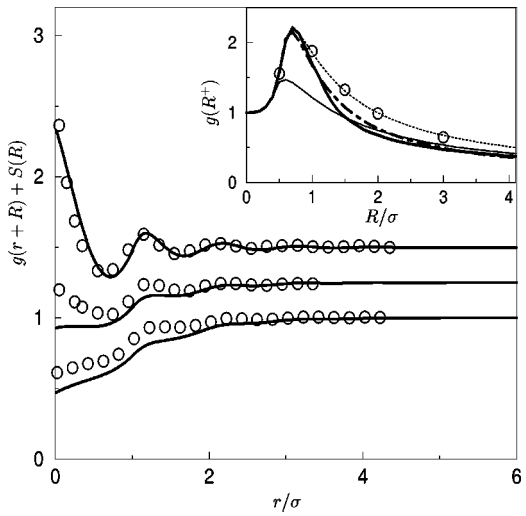

FIG. 3. Radial distribution function $g(r+R)=n(r+R)/n_l$ as a function of distance r from the cavity center for cavities with radii R of 1.0σ, 2.0σ and 3.0σ. Circles denote simulation results ($\rho^*=0.70$, $T^*=0.85$, $p^*=0.022$) and thick solid lines denote corresponding LCW theory results. For ease of viewing, the $g(r+R)$ for the cavities with radii 1.0σ and 2.0σ have been shifted vertically by 0.50 and 0.25 units, respectively [i.e., $S(R)=0$, 0.25 and 0.50 for $R=3.0\sigma$, 2.0σ and 1.0σ, respectively]. The inset shows the contact value $g(R^+)$ as a function of cavity radius R from simulation, LCW theory and three scaled particle theory calculations [using the Reiss approximation [18] (thin solid line) and the Stillinger approximation [19] with surface tension values of $0.33\varepsilon/\sigma^2$ (dot-dash line) and $0.56\varepsilon/\sigma^2$ (dotted line)]. The value of $g(R^+)$ corresponding to the density of the nearby coexisting gas is $\sim\beta p/n_l\simeq 0.04$.

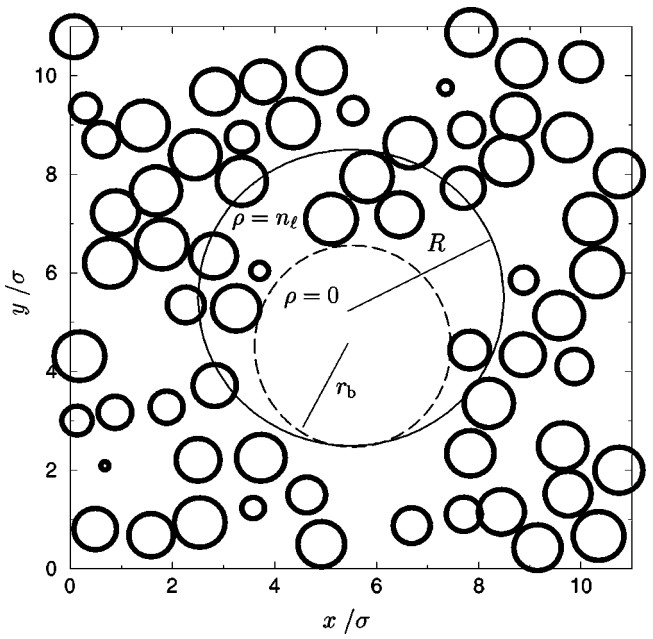

FIG. 4. Two-dimensional slice through the center of the volume with radius $R=3.0\sigma$. The heavy circles (of various sizes) are the intersections of the Lennard-Jones spheres (diameter σ) with the plane cutting the center of the volume. The positions of the spheres shows an instantaneous configuration for this slice from the simulation restricting $35\leqslant N\leqslant 40$. The circle of radius r_b depicts the vapor bubble invoked in Eqs. (5)–(7). The density ρ is zero inside the bubble and is equal to the liquid density n_l outside the bubble. The figure illustrates the assumptions used to derive Eq. (7).

for the $R=2.0\sigma$ cavity and becomes more pronounced as the size of the cavity increases. For the volumes with radii 2.0 and 3.0σ and in which N is small but nonzero, it is found that the particles inside the volume spend most of the time near the edge of the volume, illustrating the unbalanced attractive force responsible for drying [8,20]. This unbalanced force becomes significant when the size of the inhomogeneity in the solvent becomes relatively large, and counteracts the effect of the compressive force that produces the peak in $g(r)$ at contact for small cavities. For fluids without attractive interactions, such as the hard sphere fluid, $g(r)$ has a sharp peak at contact even for a large solute such as a hard wall [21].

For large volumes, the shape of the $P(N;v)$ distributions graphed in Fig. 1 for the large volumes can be explained in terms of the formation of a vapor bubble inside the volume. This model is illustrated in Fig. 4. Approximating the liquid density inside the volume but outside the bubble as the bulk liquid density n_l, N can be related to the radius of the bubble r_b, where $r_b^3=(3/4\pi n_l)(\langle N\rangle_v-N)$. The free energy required to grow the bubble is the work against a surface tension $\tilde{\gamma}$ and an external pressure p. That is,

$$F(N;r_b(N))=\frac{4\pi}{3}r_b^3p+4\pi r_b^2\tilde{\gamma}. \tag{5}$$

The probability $P(N;v)$ is the product of the Boltzmann weight for this energy and the volume accessible to the bubble inside the volume $V(N;r_b(N))=(4\pi/3)(R-r_b)^3$. Specifically,

$$P(N;v)\propto V(N)\exp[-\beta F(N)], \tag{6}$$

where $\beta=1/k_BT$. Therefore, in terms of N and the average volume occupancy $\langle N\rangle_v$,

$$\ln P(N;v)\approx \ln\{N+3\langle N\rangle_v^{1/3}(\langle N\rangle_v-N)^{1/3}[(N-\langle N\rangle_v)^{1/3}-\langle N\rangle_v^{1/3}]\}-\beta\frac{(\langle N\rangle_v-N)}{n_l}p-4\pi\beta\left(\frac{3}{4\pi n_l}\right)^{2/3}(\langle N\rangle_v-N)^{2/3}\tilde{\gamma}+(\text{const}). \tag{7}$$

Under the conditions simulated, p is small ($0.022\varepsilon/\sigma^3$) and so the second term in Eq. (7) hardly contributes to $\ln P(N;v)$. For the $R=3.0\sigma$ volume, and $N<\langle N\rangle_v/2$, the first term of Eq. (7) contributes less than 15% of the total magnitude of $\ln P(N;v)$. This entropic term does decrease sharply as $N\to 0$ and explains the corresponding downturns in the simulation curves for $\ln P(N;v)$ in Fig. 1. As the bubble grows, there are fewer ways in which it can move in the volume, resulting in a reduction in $P(N;v)$.

Most of the variation in $\ln P(N;v)$ comes from the second term. The plateau value of the quantity $\Delta\mu_v/4\pi R^2$ in Fig. 2, $0.56\varepsilon/\sigma^2$, is the free energy per unit surface area for large cavity formation. It is the surface tension for a LJ fluid adjacent to a large cavity at the thermodynamic state studied in the simulations. Using $\tilde{\gamma}=0.56\varepsilon/\sigma^2$ in Eq. (7) gives good agreement with the $P(N;v)$ distribution from simulation, as

shown in Fig. 1(d). As such, the assumption of bubble formation inside the volume appears to be physically accurate and is consistent with the occurrence of drying.

Note that the surface tension $\tilde{\gamma}$ applies to an interface constrained by the adjacent cavity wall. It should be distinguished from the surface tension, $\gamma \simeq 0.33\varepsilon/\sigma^2$, at the liquid-vapor coexisting state close to the bulk thermodynamic state considered here [13]. The surface tension $\tilde{\gamma}$ is generally larger than γ since fluctuations present in the free interface are quenched by the wall. The distinction between $\tilde{\gamma}$ and γ has been appreciated at least since the creation of scaled particle theory [22].

III. COMPARISON WITH THEORY

The simulation results described in the previous sections can be interpreted with theory, provided that theory can predict drying. Standard perturbation theories and integral equation theories such as the mean spherical approximation, the Percus-Yevick equation and so forth [23] fail in this regard because they are based upon the general model of Gaussian density fluctuations about a uniform fluid [17] . Indeed, when these theories are applied to the cavities considered in Fig. 3, they fail to predict density depletion. Instead, for $R=2.0\sigma$ and $R=3.0\sigma$, they predict density profiles similar to the $R=1.0\sigma$ case. Rather than Gaussian, an appropriate theory must be consistent with a bistable distribution for density fluctuations, with one basin of stability corresponding to a high density fluid, and the other corresponding to a low density fluid. The LCW theory [6] is a theory of this type.

The LCW theory calculations carried out in this work specifically use Eqs. (2)–(15) in Ref. [6]. To implement the theory, one needs to specify several quantities: (1) $w(n)$, the local excess density of the grand potential relative to the liquid [see Eq. (2) in Ref. [6]]; (2) γ, the surface tension of the free liquid-vapor interface at a coexistence point close to the thermodynamic state of interest; (3) λ, the length scale over which quickly varying density fluctuations, $\delta\rho(\mathbf{r})$, are coarse grained [see Eq. (14) in Ref. [6]]; and (4) $g(r)$, the radial distribution function at the bulk density n_l.

By definition,

$$w(n) = f(n) - \mu_l n - [f(n_l) - \mu_l n_l], \tag{8}$$

where $f(n)$ is the local Helmholtz free energy density of the fluid, and $\mu_l = \partial f/\partial n|_{n_l}$ is the chemical potential of the liquid. We have estimated $f(n)$ from an equation of state containing a mean field correction for the effect of truncating and shifting the LJ potential [12]. This corrected equation has been shown to accurately fit simulation data [12]. The function $w(n)$ thereby calculated using Eq. (8) is plotted as a function of n in Fig. 5. The value of the surface tension $\gamma \simeq 0.33\varepsilon/\sigma^2$ used was that determined from results of Chapela *et al.* [13] for a 2.5σ cutoff system at a temperature of $0.836 k_B T/\varepsilon$. The length scale over which the attractive interactions in the fluid fluctuate is [24]

$$\lambda = \gamma \Big/ \int_{n_g}^{n_l} dn \sqrt{2a w(n)}, \tag{9}$$

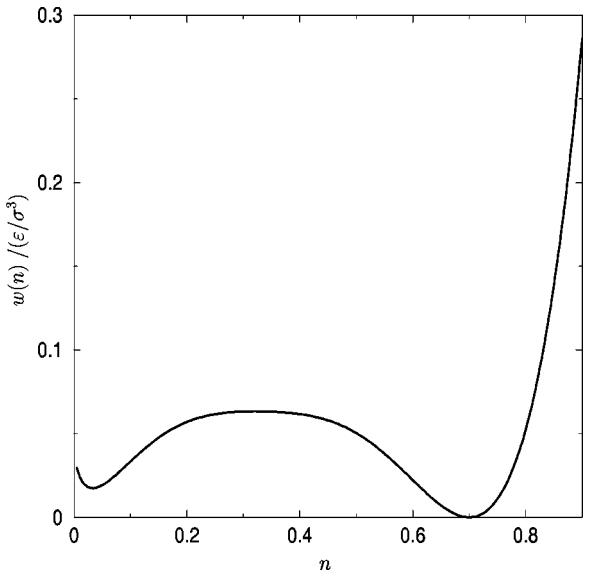

FIG. 5. Local excess density of the grand potential relative to the liquid $w(n)$ for LJ fluid at reduced liquid density $n_l = 0.70$ and reduced temperature $T^* = 0.85$.

where $a n_l^2 = -[\partial(\beta f)/\partial\beta]_{n_l}$ is the bulk energy density of the liquid. This relation gives $\lambda \simeq 0.81\sigma$. It was found that the calculations of both $P(N;v)$ and $\Delta\mu_v$ are fairly insensitive to the value of λ. Using various values of λ between 0.60σ and 1.20σ leaves $\Delta\mu_v$ virtually unchanged. The radial distribution function, $g(r)$, was obtained from computer simulation of the uniform fluid. The analytical Weeks-Chandler-Andersen approximation [15], based upon the hard sphere fluid $g(r)$, could have been used with no noticeable difference in the results we report below.

The $P(N;v)$ distributions are calculated from LCW theory using

$$P(N;v) = \frac{Z_v(N)}{\sum_{N \geqslant 0} Z_v(N)}, \tag{10}$$

where $Z_v(N)$, the partition function when N solvent molecules occupy the volume v, is given by Eq. (9) in Ref. [6]. The distributions are compared against the simulation results in Fig. 1. The cavity excess chemical potentials [Eq. (8) of Ref. [6]] are compared in Fig. 2. There is reasonable quantitative agreement between theory and simulation in both cases. The results of the theory show an approximately linear relationship between $\Delta\mu_v/4\pi R^2$ and R for the small cavities. For large values of $R, \Delta\mu_v/4\pi R^2$ is essentially a constant. The simulation results show indications of a similar plateau in $\Delta\mu_v/4\pi R^2$ for large values of R. Significantly, the value of R at which the turnover to a drying regime occurs is also reasonably well predicted by the theory.

Figure 3 shows the agreement between theory and simulation for the density profiles for cavities with radii 1.0, 2.0 and 3.0σ. The LCW calculations used $\lambda \simeq 0.81\sigma$, as suggested by Eq. (9). The profiles are qualitatively similar for λ

between 0.6 and 1.2σ. The profiles exhibit density depletion with increasing cavity size due to drying.

It is interesting to note that the plateau in $\Delta\mu_v/4\pi R^2$ calculated for water [6] occurs for cavity radii 10 Å, corresponding to a radius of 3.7σ, if the diameter of water is taken to be 2.7 Å. The turnover radius for water therefore seems to be twice as large as that found in the current study of the LJ fluid. This difference is due to the relatively large surface tension of water when compared to the LJ fluid in the thermodynamic state studied (in comparable units) [25]. The higher the surface tension, the greater cost of forming a sharp interface. As a consequence, depletion is less costly and occurs more readily for the LJ fluid than for water.

Hummer and Garde [26] examined what they termed ''weak dewetting'' by carrying out calculations for soft hydrophobic spheres in water. The spheres considered in that work produced cavities of radii $R \lesssim 5.0$ Å. As such, solvent depletion (i.e., drying) was not found in that work. Rather, these workers verified Stillinger's long standing prediction [19] that $g(R^+)$ is nonmonotonic, reaching a maximum for values of R significantly less than those that would produce drying. The presence of the maximum in $g(R^+)$ does identify the smallest cavity radius for which the effects of unbalanced forces are notable. In the inset to Fig. 2, this maximum for cavities in a Lennard-Jones fluid coincides with the evident shoulder of $\Delta\mu_v/4\pi R^2$ at $R \simeq 1\sigma$. The plateau value for this quantity, reached for $R \gtrsim 2\sigma$, is $\tilde{\gamma}$ in Eq. (7).

In light of the distinction between γ and $\tilde{\gamma}$, it is interesting to compare the simulation results and LCW predictions with those of scaled particle theory (SPT). In practice, SPT is an extrapolation or interpolation procedure that connects the chemical potentials of small and large cavities. The algebraic expressions used to make the connections are usually constructed so that $\Delta\mu_v/4\pi R^2$ exhibits a plateau when the pressure is low. Figure 2 shows the results of three such theories. The simplest, due to Reiss and co-workers [18] and applied by Pierotti to hydrophobic solvation [27], uses only small cavity properties, the pressure and average density of the fluid. When applied to the LJ fluid studied herein, it shows no plateau. Stillinger's improvement [19] upon that version incorporates in addition the variance of density fluctuations in small volumes, and an assumed surface energy, $\tilde{\gamma}$. For cavities in water, the case considered by Stillinger, γ is relatively large, making fluctuation effects relatively small and $\tilde{\gamma}$ close in value to γ [6]. Indeed, Stillinger proposed $\gamma \simeq \tilde{\gamma}$ in his SPT treatment of hydrophobicity. For the LJ fluid studied herein, however, the distinction between γ and $\tilde{\gamma}$ is important to SPT, as seen in Figs. 2 and 3. [In Fig. 3, the contact densities predicted from SPT are obtained from the SPT chemical potentials from Eq. (4)]. By adopting the LCW prediction for the value of $\tilde{\gamma}(=0.56\varepsilon/\sigma^2)$, Stillinger's SPT agrees reasonably well with the available simulation data [28]. Unfortunately, SPT provides no independent way to determine that parameter.

ACKNOWLEDGMENTS

This research has been supported in part by the National Science Foundation. Helpful discussions with Ka Lum and Lawrence Pratt are gratefully acknowledged.

[1] A. Wallqvist and B.J. Berne, J. Phys. Chem. **99**, 2893 (1995).
[2] D.E. Sullivan, D. Levesque, and J.J. Weis, J. Chem. Phys. **72**, 1170 (1980).
[3] K. Lum and A. Luzar, Phys. Rev. E **56**, R6283 (1997).
[4] K. Binder, D.P. Landau, and D.M. Kroll, Phys. Rev. Lett. **56**, 2272 (1986).
[5] R.M. Pashley, P.M. McGuiggan, B.W. Ninham, and D.F. Evans, Science **229**, 1088 (1985); H.K. Christenson and P.M. Claesson, *ibid.* **239**, 390 (1988); J.L. Parker, P.M. Claesson, and P. Attard, J. Phys. C **98**, 8468 (1994); D. Bérard, P. Attard, and G.N. Patey, J. Chem. Phys. **98**, 7236 (1993).
[6] K. Lum, D. Chandler, and J.D. Weeks, J. Phys. Chem. B **103**, 4570 (1999).
[7] P. Lijnzaad and P. Argos, Proteins: Struct., Funct., Genet. **28**, 333 (1997).
[8] J.D. Weeks, K. Katsov, and K. Vollmayr, Phys. Rev. Lett. **81**, 4400 (1998).
[9] G. Hummer, S. Garde, A.E. García, A. Pohorille, and L.R. Pratt, Proc. Natl. Acad. Sci. USA **93**, 8951 (1996).
[10] G. Hummer, S. Garde, A.E. García, M.E. Paulaitis, and L.R. Pratt, J. Phys. Chem. B **102**, 10 469 (1998)
[11] M.A. Gomez, L.R. Pratt, G. Hummer, and S. Garde, J. Phys. Chem. B **103**, 3520 (1999).
[12] J.K. Johnson, J.A. Zollweg, and K.E. Gubbins, Mol. Phys. **78**, 591 (1993).
[13] G.A. Chapela, G. Saville, S.M. Thompson, and J.S. Rowlinson, J. Chem. Soc., Faraday Trans. 2 **8**, 1133 (1977).
[14] C.D. Hollcomb, P. Clancy, and J.A. Zollweg, Mol. Phys. **78**, 437 (1993).
[15] J.D. Weeks, D. Chandler, and H.C. Andersen, J. Chem. Phys. **54**, 5237 (1971).
[16] D. Frenkel and B. Smit, *Understanding Molecular Simulation: From Algorithm to Applications* (Academic Press, San Diego, 1996).
[17] D. Chandler, Phys. Rev. E **48**, 2898 (1993).
[18] H. Reiss, H.L. Frisch, and J.L. Lebowitz, J. Chem. Phys. **31**, 369 (1959).
[19] F.H. Stillinger, J. Solution Chem. **2**, 141 (1973).
[20] J.D. Weeks, R.L.B. Selinger, and J.Q. Broughton, Phys. Rev. Lett. **75**, 2694 (1995).
[21] R.D. Groot, N.M. Faber, and J.P.v.d. Eerden, J. Chem. Phys. **62**, 861 (1987).
[22] H. Reiss, H.L. Frisch, E. Helfand, and J.L. Lebowitz, J. Chem. Phys. **32**, 119 (1960).
[23] J. P. Hansen and I. R. McDonald, *Theory of Simple Liquids* (Academic Press, London, 1986).
[24] This equation for λ coincides with the relationship $\lambda = \sqrt{m/a}$ used in Ref. [6].
[25] Taking the value of σ for water to be 2.7 Å, the ratio of the

surface energy $\gamma\sigma^2$ to the bulk energy per particle an_l is 0.25 and 0.078, respectively, for water and the LJ fluid.
[26] G. Hummer and S. Garde, Phys. Rev. Lett. **80**, 4193 (1998).
[27] R.A. Pierrotti, J. Phys. Chem. **69**, 281 (1965).
[28] Stillinger's theory requires the specification of a shell length. In the application of his theory, illustrated in Figs. 2 and 3, we have assigned 0.58σ as the value of this length. This value was chosen because our simulation results show that density cumulants of higher order than the variance contribute significantly to $P(N;v)$ only for cavities with radii larger than this size.